

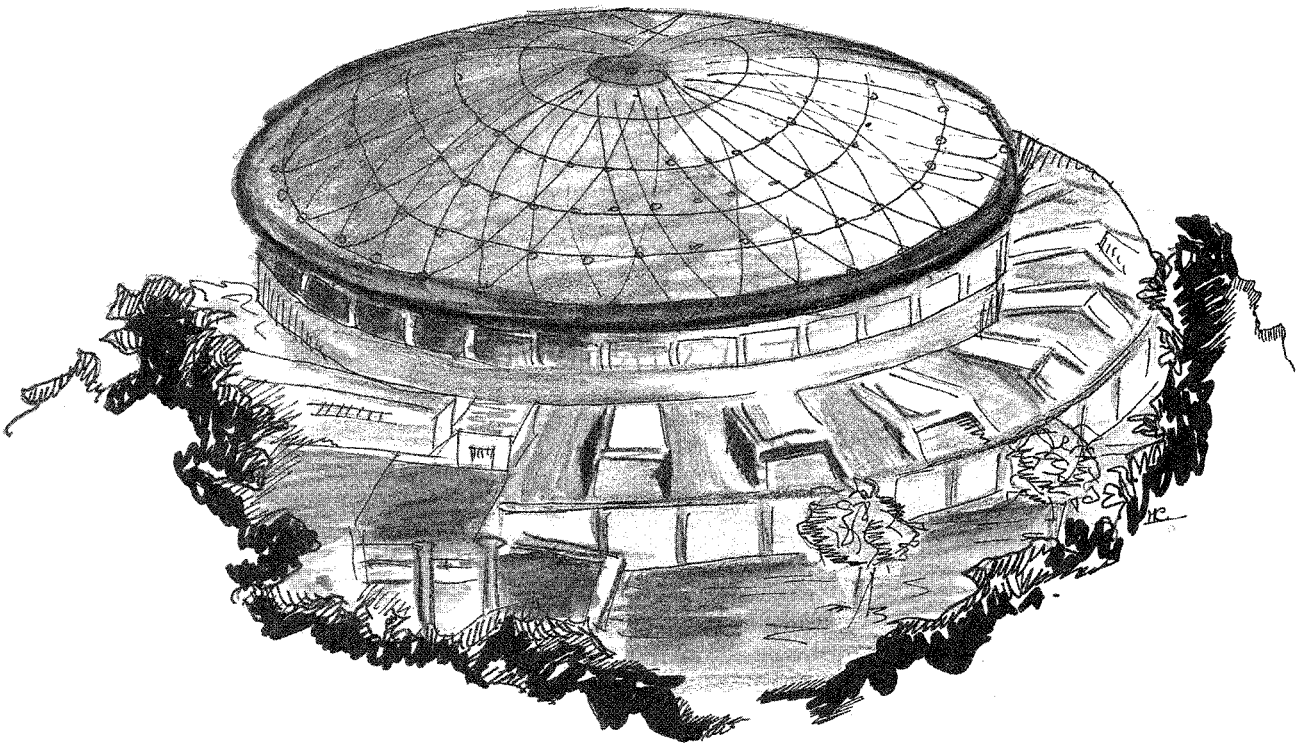


# Laboratori Nazionali di Frascati

LNF-89/064(R)  
28 Settembre 1989

D. Di Gioacchino, U. Gambardella, P. Gislon, G. Paternò, C. Vaccarezza:

**SUPERCONDUCTING PROPERTIES OF NIOBIUM THIN FILMS FOR  
APPLICATIONS IN ACCELERATING CAVITIES**



Servizio Documentazione  
dei Laboratori Nazionali di Frascati  
P.O. Box, 13 - 00044 Frascati (Italy)

**SUPERCONDUCTING PROPERTIES OF NIOBIUM THIN FILMS FOR  
APPLICATIONS IN ACCELERATING CAVITIES**

D. Di Gioacchino, U. Gambardella, P. Gislou\*, G. Paternò\*, C. Vaccarezza  
I.N.F.N. - Laboratori Nazionali di Frascati, P.O. Box 13, 000044 Frascati (Rome), Italy

**Abstract**

The use of bulk Niobium in superconducting cavities is at present the easiest way to realize those devices, especially for the applications in particle accelerators such as our LIS-A machine. However for the future applications requiring higher performances of these active devices the actual bulk Niobium technology suffers some limitations, which may be only in part overcome. Thus, following the CERN experience, we began to study, in the framework of the ARES program, the applications of thin film technology to the superconducting cavities. We fabricated several Niobium thin films, by means of our dc magnetron sputtering deposition system, on a planar glass substrate at ambient temperature. For each sample we measured the resistance versus temperature dependence down to the transition temperature, and the transition temperature behavior as a function of the applied magnetic field up to 5 Tesla. The results indicate that, although the very first samples showed an higher residual resistance and a lower transition temperature, we were able to get rather good quality Niobium thin films having transition temperatures higher than 9.24 K.

**1 - Introduction**

Nowadays superconducting cavities are being used in many particle accelerators for their higher efficiency as active devices compared to normal cavities. This feature in addition allows to obtain a beam having better characteristics, such as low energy spread. Also at LNF there is in progress the realization of the LIS-A linear accelerator using superconducting cavities operated at 500 MHz (1). The standard bulk Niobium technology was adopted as a first approach, whilst

---

\* E.N.E.A. - C.R.E. Frascati, P.O. Box 65, 00044 Frascati (Rome), Italy

future developments are foreseen. The use of bulk Niobium is favored because of its relatively high critical temperature  $T_c \approx 9.2$  K, and its good mechanical properties compared to other superconducting metals. Moreover the upper critical field  $H_{c2} \approx 1600$  Gauss at 4.2 K of pure Niobium and its surface resistance  $R_s$  calculated from BCS theory at 500 MHz and 4.2 K, lead to a theoretical limit for the corresponding accelerating electrical field  $E_a \approx 40$  MV/m and to a quality factor  $Q_0 \approx 4 \times 10^9$ .

Unfortunately the accelerating fields routinely achieved in Niobium sheet cavities at 500 MHz and 4.2 K do not exceed 10 MV/m, with a  $Q_0$  value of  $1 \times 10^9$  (2).

In order to get higher  $Q_0$  values in correspondence of higher  $E_a$  fields, cavities could be operated at temperatures lower and lower, because in agreement to the BCS theory of superconductivity we should have, in the limits described in (3),  $R_s \propto \omega^2 \rho_n^{1/2} e^{-(1.76/t)}$ , where  $t = T/T_c$  is the reduced temperature,  $\omega$  is the frequency, and  $\rho_n$  is the normal state resistivity.  $R_s$  for real superconductors follows this temperature behavior only up to a certain value, where a saturation effect is always found. This final value is usually called residual resistance  $R_{res}$ , and it is mainly accounted for both impurities (4) and temperature independent loss mechanisms (5) occurring on the cavity surface in the presence of the electromagnetic field. At present there is not an exhaustive theory which can predict the  $R_{res}$  value for a superconductor.

One of the limits of superconducting cavities made of bulk Niobium is the relatively poor thermal conductivity, which reduces the heat exchange between the inner cavity surface (where the loss mechanisms generate the heat) and the outer surface (where the heat is absorbed by the helium bath). The dissipated power on the inner surface is (6):

$$P = \frac{R_s}{2 \mu_0^2} \int_s B^2 dS$$

being  $R_s$  the real part of the surface impedance,  $B$  the induction field and  $\mu_0$  the magnetic permeability of vacuum. This power has to be compared (7) to the heat flux density

$$Q = (k_{Nb} / d) (T_i - T_B)$$

where  $k_{Nb}$  is the Niobium thermal conductivity,  $d$  the wall thickness of the cavity,  $T_i$  and  $T_B$  respectively the inner surface temperature and the outer bath temperature. This rule is true only when the heat density flow is lower than the value which generates local film boiling effect. The higher is the residual resistivity ratio RRR the higher is the  $k_{Nb}$ . In practice it is usual to find small non superconducting parts on the inner cavity surface which exhibit enhanced surface impedance. Consequently there is a larger heat generation, that may induce a thermal breakdown of the whole cavity even at relatively low values of  $E_a$ . To identify the presence of "hot spots" a particular technique is usually adopted (8) called temperature mapping. It has been reported (9) that with  $E_a \approx 10$  MV/m the critical diameter of  $72 \mu\text{m}$  of a normal impurity can induce a thermal breakdown in a cavity made of RRR=40 Niobium ( $k_{Nb} \approx 5 \text{ Wm}^{-1}\text{K}^{-1}$ ) while using the RRR=300

Niobium quality ( $k_{\text{Nb}} \approx 50 \text{ Wm}^{-1}\text{K}^{-1}$ ) the critical diameter increases up to 480  $\mu\text{m}$ . Thus the cryogenic stabilization due to the high conductivity Niobium may be a good key to get higher  $E_a$ , but with the corresponding higher losses. The effect of the RRR value on the field is  $E_a \propto (\text{RRR})^{1/2}$ , but it is to be considered that the mechanical properties of the Niobium, i.e. yield strength, elongation, etc., decrease with the purity. This implies that for larger cavities, i.e. at lower frequencies, very high value of RRR may lead to an increase of the wall thickness for mechanical stability. Moreover computer simulations (10), theoretical calculations (11), and some data (12) show that the BCS surface resistance increases increasing the RRR. In practice this means that the  $Q_0$  value decreases increasing the Niobium purity, and this effect is more evident at lower frequencies (13). Taking into account that the RF electromagnetic fields do not penetrate within the bulk material, the use of a superconducting thin film deposited within a copper cavity should realize a superconducting cavity having the same good thermal conductivity of copper ( $k_{\text{Cu}} \approx 400 \text{ Wm}^{-1}\text{K}^{-1}$  for copper ETP @ 4.2 K). This idea has been pursued by C. Benvenuti and co-workers (14, 15), and actually they have shown the feasibility of LEP superconducting cavities at 350 MHz by using a sputtering technique within the four cell cavity. Furthermore it has experimentally been observed that for these cavities the  $Q_0$  value at low fields is independent of the earth magnetic field (16). This feature allows to avoid the compensation system of the magnetic field during the normal superconducting transition. Also it has to be noticed that for this kind of cavities the  $Q_0$  value at low field is always higher than the  $Q_0$  measured in the same cavities made of bulk Niobium. This is probably due both to the lower RRR of the Niobium thin film (in the range 20 - 40), and to the weak effect of the magnetic field on the Nb/Cu superconducting cavities (15).

Here we report preliminary results we got in fabricating Niobium thin films and a summary of their superconducting properties we measured. In sec. 2 the fabrication process is summarized. In sec. 3 the experimental set up and the results on the  $T_c$  measurements are reported, both in the absence and in the presence of strong magnetic fields. The experimental data are discussed in terms of sample impurity contents related to the fabrication process. Brief conclusions are given in sec. 4.

## 2 - Thin film fabrication

We have realized the Niobium films by using the Leybold L 560 thin film fabrication plant which is equipped with a 3" Nb cathode. Though our system allows for both RF and DC magnetron sputtering, we preferred the last one in view of the good metallic behavior of Nb. The evacuation system consists of a fore vacuum group (two stage rotary pump 75  $\text{m}^3/\text{h}$  plus a mechanical roots 500  $\text{m}^3/\text{h}$ ) and a turbo molecular pump having 1000 l/s pumping speed. This pumping unit allows to reach a final vacuum of in the low range of  $10^{-7}$  mBar in few hours. All the samples have been deposited through a steel mask, to get a linear strip approximately  $20 \times 2.2 \text{ mm}^2$ , on a Corning 7059 glass substrate, without any substrate heater. The substrates have

previously been cleaned by using the commercial Balzers substrate cleaner products, and then placed into the vacuum chamber. The film growth has been monitored by using the quartz thickness monitor Inficon XTC. A summary sketch of the sputtering chamber is in Fig. 1. The first group of samples has been processed as follows:

- a. vacuum into the chamber before the deposition  $2\text{--}3 \times 10^{-7}$  mBar;
- b. introduction of Ar gas up to reach a pressure of  $5 \times 10^{-3}$  mBar;
- c. 5 minutes long pre sputtering at 100 W while the substrate is kept far from the cathode;
- d. sputtering on the glass substrate up to get a nominal thickness of 3'000 Å, both at 400 W and at 550 W.

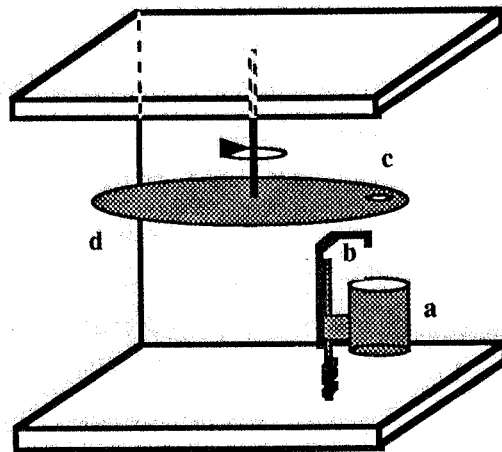


FIG. 1 - Sputtering chamber overview.

- a) target
- b) thickness monitor
- c) substrate holder seat
- d) rotating plate

Step a has usually been reached by pumping within the chamber for 12 hours overnight. No bake out has been performed during this time, though the plant is designed for circulation of warm water in the vacuum chamber walls. Moreover we have not used any cold trap on the turbo pump. The Ar gas N60 quality (99.9995 %) has been introduced through either a leak valve or a mass flow controller; in the latter case the inlet gas comes in directly in the proximity of the substrate. With the dc power off the mass flow rate to get  $5 \times 10^{-3}$  mBar is about 75 sccm. The pre sputtering is intended to remove oxides from the cathode surface. The rate of growth on the substrate side is about 2 Å/s at 100 W, and respectively 7 and 9 Å/s at 400 and 550 W.

After the measurements on samples of this group we decided to increase both the pre sputtering time and rate. This was for a deeper etching of the cathode surface, and for a better adherence of the film on the substrate. The dc power used was 600 W, for both the pre sputtering and the deposition. The deposition rate was  $\approx 9.6$  Å/s and the film final thickness was increased to 6000 Å. The pre sputtering lasted more than 20 minutes. We also used a worse Ar quality (99.9985%) in this second group of samples.

Finally for the last depositions we changed the steel mask, whose geometry is reported in Fig. 2, which should allow us to measure more precisely the electric parameters of the film. The deposition rate of this set was 6.5 Å/s at beginning, and 9.5 Å/s later on.

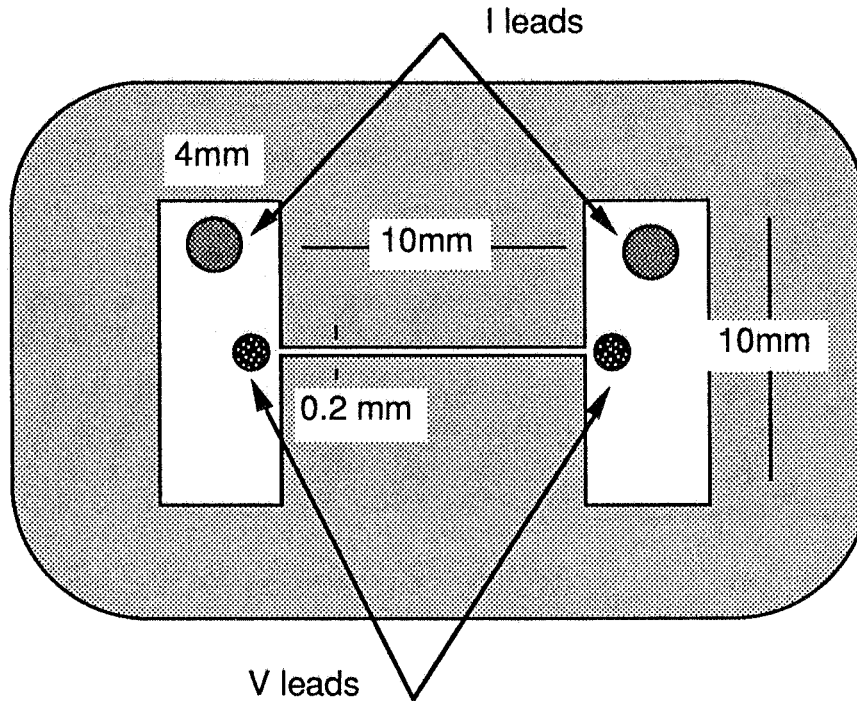


FIG. 2 - Stainless steel mask geometry.

### 3 - Experimental results

All the measurements have been performed in a gas flow variable temperature cryostat provided with a superconducting magnet able to generate a magnetic field up to 5 T. The samples are fixed on a bulk copper sample holder with the film plane parallel to the generated magnetic field. The resistances have always been measured by using a four leads configuration. A scheme of the measurements instruments is reported in Fig. 3. We took care of the current density value, low enough to neglect for each measurement the resistive self heating, the magnetic self field and the critical current density. During the cool down the automatic data acquisition system enabled, at fixed temperature intervals, the 1 mA constant bias current to flow into the sample and soon after it took the voltage across the sample. We arranged, by software control, the double voltage reading both with direct and inverse current flow in order to avoid the fluctuating thermal emf. The temperature has been measured by means of a Lake Shore calibrated carbon glass resistor (CGR), fed at constant current of 10  $\mu$ A, and placed in close thermal contact with the sample. The resistance value has been interpolated to get the temperature by using the standard relation (17):

$$\log(R) + K / \log(R) = A + B / T$$

where  $R$  is the CGR resistance,  $T$  is the temperature, and  $K$ ,  $A$ , and  $B$  are constants to be determined from the calibration points. We applied this relation to fourteen ranges of temperature to get a precision of  $\pm 0.05$  K in the range of our interest. Moreover in order to guarantee a good

thermal equilibrium between the sample and the thermometer the rate of temperature variation near the superconducting transition has been kept as low as 0.1 K/min.

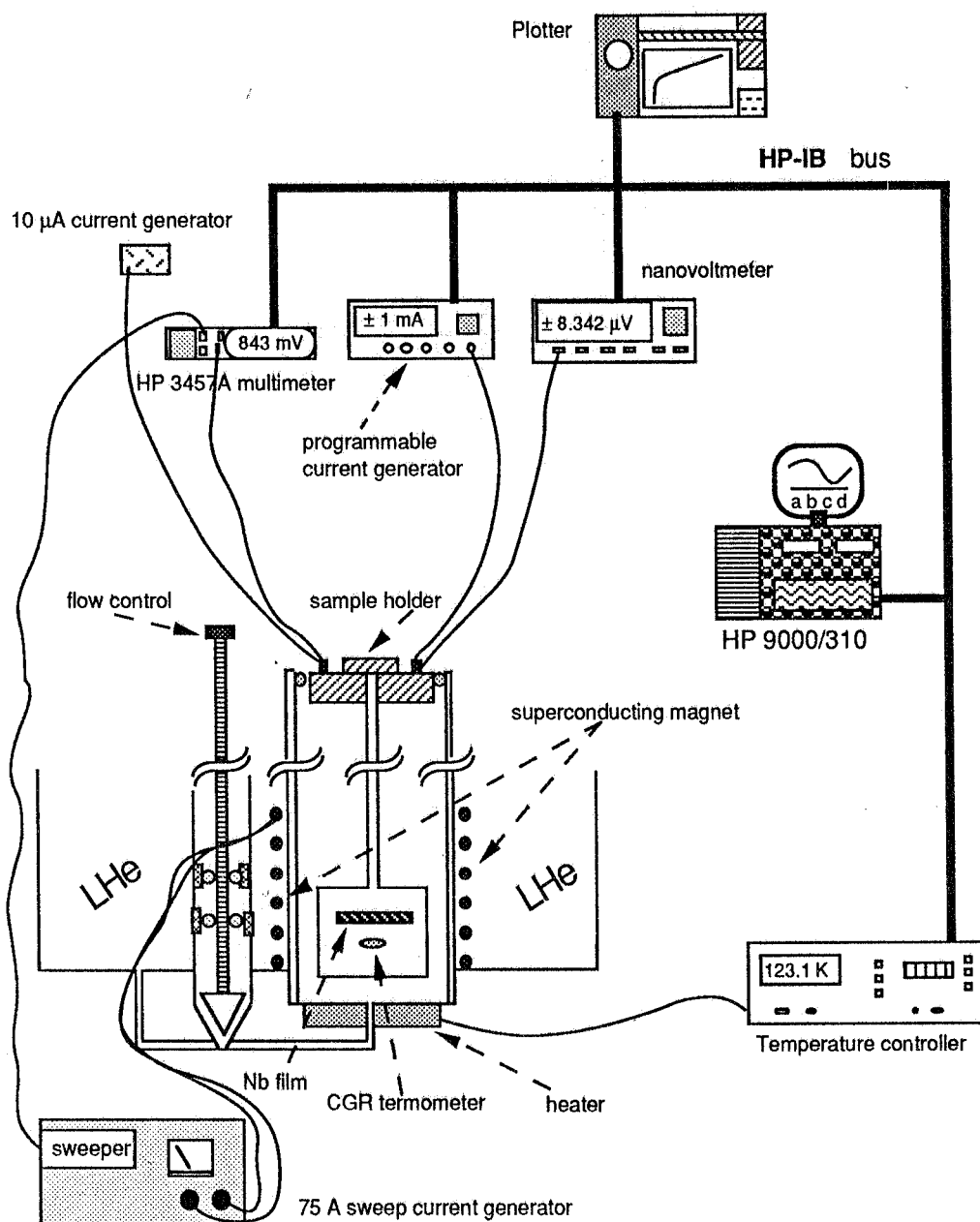


FIG. 3 - Block scheme of the measuring instruments.

In Table I the main electric features of two representative samples for different sputtering conditions are reported. Here  $\beta$  is the sample resistivity ratio between the room temperature and the indicated one. In this table  $T_c$  is defined as the temperature corresponding to the half value of the resistive transition. The transition amplitude  $\Delta T_c$  is here intended as the temperature difference between the transition onset and the zero resistance value. It is mainly due to the minimum temperature increment we recorded, so that the real transition amplitude must be equal or smaller. A measure of resistivity is made on the first sample of the last group whose geometry

was well defined and its thickness of 4000 Å has been measured by a profilometer. For this film we got 19.6  $\mu\Omega$  cm at ambient temperature and 8.9  $\mu\Omega$  cm at L N<sub>2</sub>.

TABLE I

|         | $\beta_{77}$ | $\beta_{10}$ | $T_c$ (K) | $\Delta T_c$ (K) |
|---------|--------------|--------------|-----------|------------------|
| group 1 | 2.4          | 3.5          | 9.05      | 0.15             |
|         | 2.4          | 3.5          | 9.05      | 0.14             |
| group 2 | 2.7          | 4.7          | 9.24      | 0.10             |
|         | 2.6          | 4.6          | 9.18      | 0.10             |
| group 3 | 2.2          | -            | -         | -                |
|         | 2.5          | 4.53         | 9.15      | 0.10             |

However the resistivity values we roughly measured on the two best samples, belonging to group 2, taking into account of the space between the voltage leads and the nominal thickness is about 13  $\mu\Omega$  cm ( $\pm 20\%$ ) at ambient temperature and 4  $\mu\Omega$  cm at 10 K. This value is comparable with 2-4  $\mu\Omega$  cm reported for Niobium films (18,19) and 3.6  $\mu\Omega$  cm at 10 K for bulk Niobium having  $\beta = 6$  (20). In Fig. 4 the typical behavior of the resistance versus the temperature of our superconducting films is reported in the whole range 300  $\div$  4.2 K.

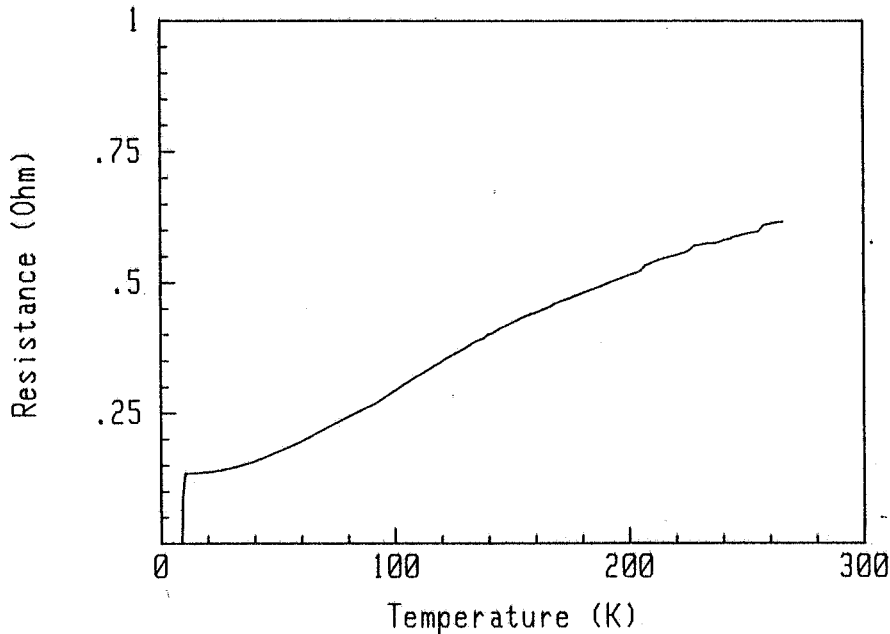


FIG. 4 - Typical R - vs - T dependence of our Niobium films.

The resistance decreases with temperature in the range 300 < T < 40 K showing a decrease as  $T^n$  with  $n < 1$ , i.e. not perfectly linear; this effect observed in all our Niobium films at higher temperatures may be related to the presence of the strong coupling factor  $\lambda$  between electrons and phonons (21). The lowering of the temperature below 40 K leads to a gradual saturation of the



resistance, which reaches a constant value called residual resistance. This resistance is evidenced when  $T \ll \Theta_D$  ( $\Theta_D$  = Debye temperature  $\approx 320$  K for Niobium) where the electronic scattering with lattice becomes negligible, while the scattering due to the impurities, temperature independent, is the main contribution to the resistivity. As can be deduced from data in Table I the highest temperature transitions correspond to the highest  $\beta$  values, and also to the lowest resistivities. Thus, according to ref.19, the measure of  $\beta$  at low temperature is an immediate test of the film quality from the point of view of impurity contents.

In Fig. 5 the typical resistive transitions in the presence of magnetic field are reported. These data have been recorded always decreasing the temperature with fixed static magnetic fields. This is a measure of the Niobium upper critical field  $H_{c2}$  at different temperatures and it can be related to the impurities present in the Niobium (22). From these records it is evident a strong effect of the field on the transition amplitude. This can be due both to flux motion induced dissipation, and to granular structures.

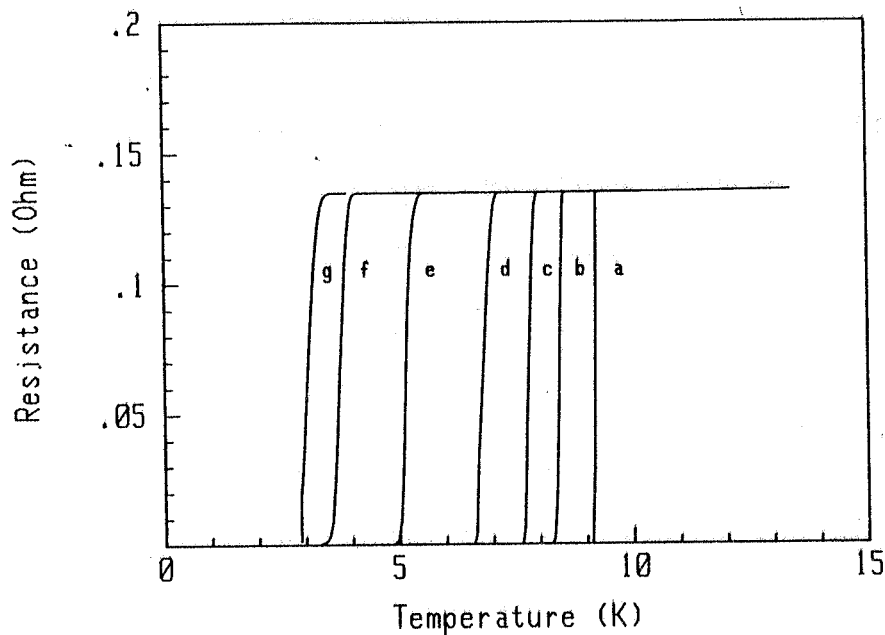


FIG. 5 - Typical resistive superconducting transitions in the presence of parallel magnetic field: curve a)  $B = 0$  Gauss; curve b)  $B = 440$  Gauss; curve c)  $B = 1150$  Gauss; curve d)  $B = 2300$  Gauss; curve e)  $B = 5000$  Gauss; curve f)  $B = 10000$  Gauss; curve g)  $B = 15000$  Gauss.

In Fig. 6 the  $H_{c2}$  - vs -  $T$  behavior of three different films, respectively belonging to the first, second, and third series, are reported. The measured critical fields in some case are as high as 4 Tesla at 3 K! The rate of decrease of  $H_{c2}$  is about 3.3 kG/K near  $T_c$ . Our results indicates the critical field of Niobium films is much higher than the bulk critical field, as reported also from other experiments (23).

From a comparison between our measurements with data reported in ref.24 it results that the initial slope shown in Fig. 6 of the  $H_{c2}$  with the temperature is close to the indicated  $dH_{c2}/dT$  for Nb films having the same thickness. Moreover the reported values of  $H_{c2}$  at low temperatures

are in the same range we found for our films, i.e. several tens of kG. In order to look for a suitable relation of the temperature dependence of  $H_{c2}$ , the Abrikosov relation for type II superconductors may be used:

$$H_{c2} = \sqrt{2} \kappa H_{cb}$$

where  $\kappa$  is the Ginzburg-Landau parameter and  $H_{cb}$  is the "bulk" thermodynamic critical field.

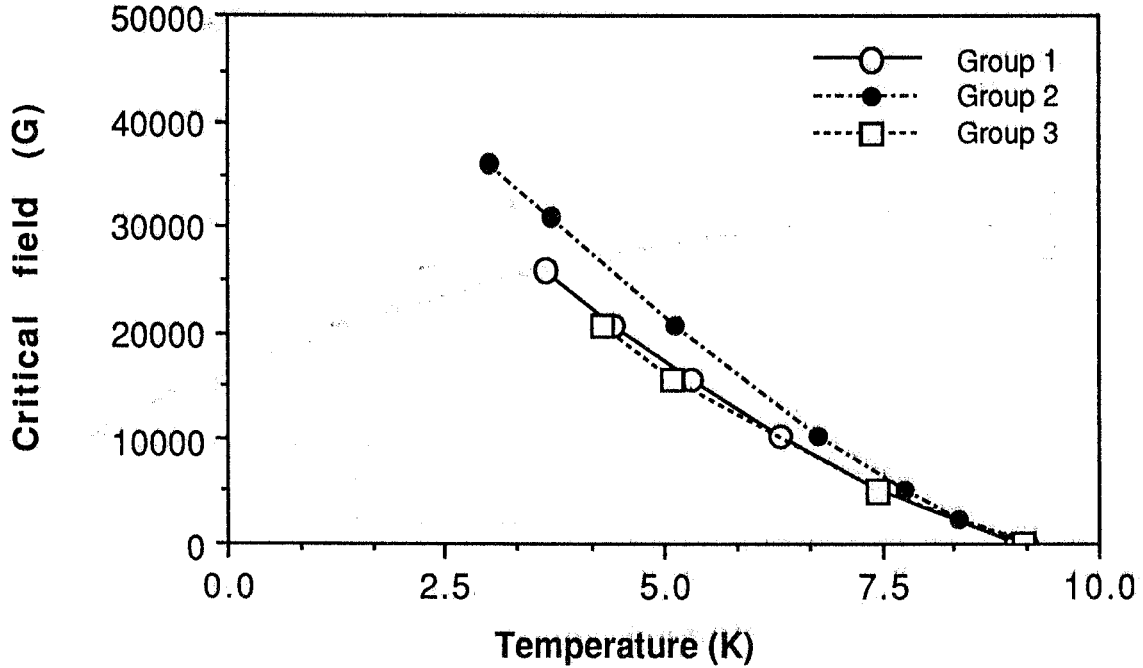


FIG. 6 - Experimental behavior of the upper critical field as a function of the temperature for films belonging to different groups. Dotted lines are only to connect homogeneous data.

The temperature dependence is both in the  $H_{cb}$  and in the parameter  $\kappa = \lambda(T) / \xi(T)$ , where  $\lambda(T)$  is the magnetic penetration depth and  $\xi(T)$  the coherence length. There are several formulations for the theoretical  $H_{c2}(T)$  curve (25, 26, 27) taking into account of the bulk material different conditions.

The Gor'kov analysis indicates two contributions to  $\kappa = \kappa_0 + \kappa_1$ , being  $\kappa_0$  the contribution of the electronic structure, and  $\kappa_1$  related to the mean free path. If we consider we are in the thick film limit, that is when the sample thickness is larger than the effective coherence length, we can write (28)  $\kappa_1$  as  $\kappa_1 \approx 7.53 \times 10^3 \sqrt{\gamma \rho_n}$ , where  $\gamma$  is the Sommerfeld constant, and:

$$H_{c2} = \sqrt{2} H_{cb} (\kappa_0 + 7.53 \times 10^3 \sqrt{\gamma \rho_n})$$

Being for thermodynamic considerations  $H_{cb} = (2\pi \gamma)^{1/2} T_c (1 - t^2)$ , it is possible to get the  $H_{c2}(T)$  curve with the parameter  $\kappa_0(T)$ . Measurement (25) of the temperature dependence of  $\kappa_0(T)$  gives a linear fit  $\kappa_0 = 1.59 - 0.72 t$ . In Fig. 7 is shown a plot of the theoretical  $H_{c2}(T)$  together with some experimental data measured on a sample of group 1. The values of  $\rho_n = 6 \mu\Omega$

cm and  $T_c = 9.24$  K have been used to compute the theoretical points. Though the data are well fitted by theory in the Ginzburg-Landau limit, i.e. when  $T$  approaches  $T_c$ , lowering the temperature there is a completely different behavior. This may be accounted for because in a thin film other effects play an important role in determining both  $H_{c2}$  and its behavior with temperature. In fact a strong dependence on the film grain size of the value of  $H_{c2}$  is reported (24).

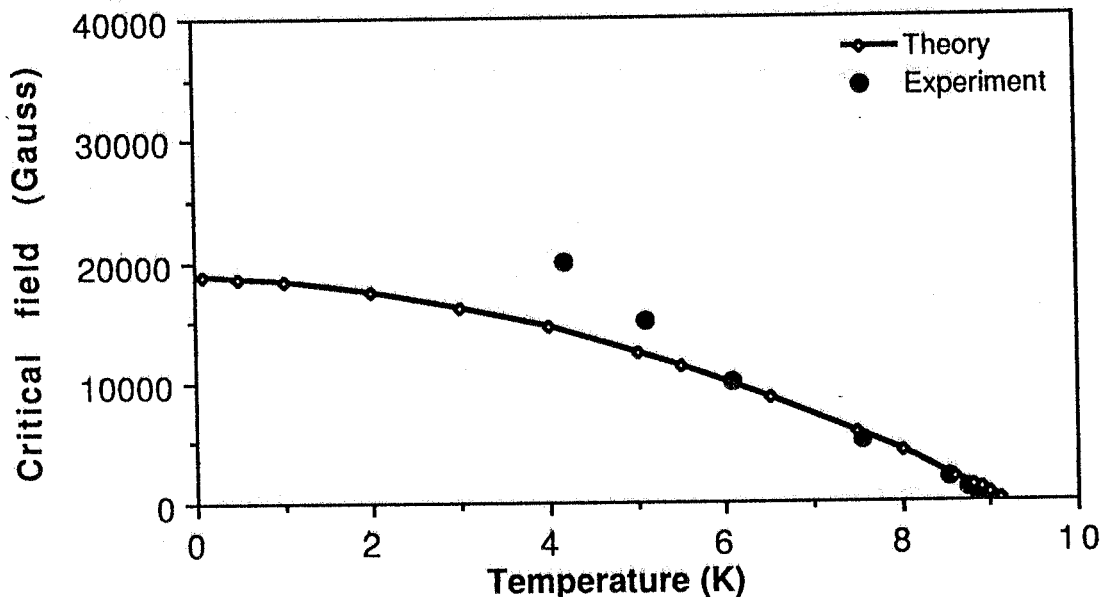


FIG. 7 - Comparison between expression (1) calculated with  $T_c = 9.24$  K,  $\rho_n = 6$   $\mu\Omega$  cm, and experimental data.

#### 4 - Conclusion

The fabrication of superconducting cavities by means of a superconducting thin film in a copper cavity seems to have good perspectives for the requirements of accelerating cavities with higher performances. In this framework we are pursuing studies on the fabrications of thin films looking to their superconducting properties. The first approach concerns Niobium thin films, which for their known properties allow a better comparison with reported data. Moreover we analyzed the behavior of the upper critical field as a function of temperature, which is also related to the sample impurity content. The data are fitted with the Abrikosov relation in the Ginzburg Landau limit, but far from the critical temperature the agreement with the theory for bulk samples is lost. However our results are similar to measurements reported into literature, which suggest that other effects are dominant in the  $H_{c2}(T)$  curve for Niobium films. To have a deeper understanding on the  $H_{c2}(T)$  behavior further experiments have to be carried out to relate in addition the effect either of the film thickness or of the film grain size on the  $H_{c2}(T)$  curve. To check for these parameters on the  $H_{c2}(T)$  for a Niobium thin film a new fabrication set-up is being realized, which includes a better vacuum in the chamber, the use of a fixed mask, and a substrate heater.

## References

1. A. Aragona *et al.*, Proc. LINAC-88 Conf., to be published.
2. H. Lengeler, CERN internal note CERN/EF 86-15 (1986).
3. H. Piel, "Basic features of superconducting RF cavities", University of Wuppertal internal note WUB 87-13 (1987).
4. J. Halbritter, "Comparison between measured and calculated RF losses in the superconducting state", Z. Physik 238, p. 466-476 (1970).
5. J. Halbritter, "On Rf residual losses in superconducting cavities", Proc. 2nd Workshop on RF Superconductivity, H. Lengeler Ed., Geneva, July 23-27, 1984.
6. H. Pfister, "Superconducting Cavities", Cryogenics, p.17-24 (January 1976).
7. N. Krause, B. Hillenbrand, Y. Uzel, K. Schnitze, Appl. Phys. A 30, p. 67-71 (1983)
8. G. Muller, "Diagnostic techniques and defect classification", Proc. 2nd Workshop on RF Superconductivity, H. Lengeler Ed., Geneva, July 23-27, 1984.
9. M. G. Oravec, B.Y. Yu, K. Riney, L. W. Kessler, and H. Padamsee, "High-speed automated NDT device for Niobium plate using scanning laser acoustic microscopy", Proc. 3rd Workshop on RF-Superconductivity, ANL-PHY-88-1, Argonne, Sept. 14-18, 1987.
10. E. Martinez, H. Padamsee, SRF 841201-EX (1984).
11. F. Palmer, CLNS 87/106 (1987).
12. H. Lengeler, Technical note EF/RF, CERN/EF/4130H/HL/mnb, 3 Oct. 1988.
13. Y. Kojima, Proc. XIth Int. Conf. Cyclotrons and their Applications, Tokyo, Oct. 13-17, 1986.
14. C. Benvenuti, N. Cirelli, M. Hauer, W. Weingarten, "Superconducting 500 MHz accelerating copper cavities sputter coated with Niobium films", Proc. 2nd Workshop on RF Superconductivity, H. Lengeler Ed., Geneva, July 23-27, 1984.
15. C. Benvenuti, D. Bloess, E. Chiaveri, N. Hilleret, M. Minestrini, W. Weingarten, "Preparation of Niobium coated Copper superconducting RF cavities for the Large Electron Positron collider", Proc. 1st EPAC Conf., S. Tazzari Ed., Rome 7-11, 1988
16. G. Arnolds-Meyer, W. Weingarten, IEEE Trans. Magn. on Mag, 24, 1621 (1987).
17. G. K. White, "Experimental Techniques in Low Temperatures Physics", Clarendon Press, Oxford, 1979.
18. R. Di Leo, A. Nigro, G. Nobile, R. Vaglio, "Niobium-Titanium nitride thin films for superconducting RF accelerating cavities", to be published in Jour. Low Temp. Phys.
19. G. Costabile, A. M. Cucolo, V. Fedullo, S. Pace, R. D. Parmentier, B. Savo, R. Vaglio, "Progress on niobium-based Josephson junction technology", Università di Salerno Internal Report 87/77 (1977).
20. S. H. Autler, E. S. Rosenblum, K. H. Goen, "High-field superconductivity in Niobium", Phys. Rev. Lett. 9, 12, 489 (1962).
21. M. Gurvitch, "What can be learned from the normal state resistivity ?", Physica 135B, 276 (1985).
22. W. De Sorbo, "Effect of dissolved gases on some superconducting properties of Niobium", Phys. Rev. 132, 1, 107 (1963).
23. I. G. D'Yakov, B. G. Lazarev, A. A. Matsakova, O. N. Ovcharenko, "Critical magnetic field of superconducting Niobium films", Sov. Phys. JETP 19, 3, 568 (1964).
24. J. J. Hauser, H. C. Theuerer, "Size effects in thin films of  $V_3Ge$ , Nb, and Ta", Phys. Rev. 134, 1A, 198 (1964).
25. S. H. Autler, E. S. Rosenblum, K. H. Goen, "The dependence of the upper critical field of Niobium on temperature and resistivity", Review of Modern Physics, p. 77 (January 1964).
26. C. K. Jones, J. K. Hulm, B. S. Chandrasekar, "Upper critical field of solid solution alloys of the transition elements", Review of Modern Physics, p. 74 (January 1964)
27. T. G. Belincourt, R.R. Hake, "Superconductivity at high magnetic fields", Phys. Rev. 131, No. 1, 140 (1963).
28. B. B. Goodman, IBM J. Res. Develop. 6, 63 (1962).